Eur. Phys. J. Special Topics **224**, 289–298 (2015)

DOI: 10.1140/epjst/e2015-02360-8

THE EUROPEAN PHYSICAL JOURNAL SPECIAL TOPICS

Regular Article

Effect of liquid bridge shape on the oscillatory thermal Marangoni convection

T. Yano[a] and K. Nishino[b]

Department of Mechanical Engineering, Yokohama National University, 79-5 Tokiwadai, Hodogaya-ku, Yokohama, Kanagawa 240-8501, Japan

Received 31 July 2014 / Received in final form 16 February 2015
Published online 8 April 2015

Abstract. The effect of liquid bridge shape on the instability and associated oscillation mode of Marangoni convection due to the temperature gradient along the free surface is experimentally studied. Although the onset condition of oscillatory state is known to depend on the liquid bridge shape, this effect is not completely understood yet. Onset conditions are measured for various combinations of the aspect ratio (AR) and the volume ratio (VR) of liquid bridges. It is found that the convection becomes most stabilized at a certain combination of AR and VR and also that the oscillation mode changes at this most stabilized condition. To account for the effects of AR and VR in a simple way, a new dimensionless parameter SDR (i.e., the ratio of the surface length to the neck diameter) is proposed. It is shown that all the onset conditions measured presently are well correlated with SDR.

1 Introduction

Marangoni convection is driven by the temperature gradient along the free liquid-gas interface. The flow is usually driven from higher temperature side toward lower temperature side. This flow plays an important role in small scale phenomena because the surface force becomes dominant over the body force as a result of the decrease of the length scale. The flow geometry considered in this study is a half-zone (HZ) liquid bridge (LB, hereafter) suspended between coaxial disks with different temperatures (Fig. 1a). This flow geometry is simplified from the floating-zone (FZ) method (Fig. 1b), which is known as a high purity crystal growth technique. The flow in the HZ LB remains steady and laminar if the temperature difference is small, while it becomes oscillatory and three-dimensionally complex if the temperature difference exceeds a certain level, which is represented by the critical temperature difference and the oscillation frequency.

It is well recognized that the onset of oscillatory flow depends on various parameters such as physical properties of the fluid, the length and the volume of the LB, heat exchange through the liquid surface and so on. Hu et al. [1] and Masud

[a] Research Fellow of Japan Society for the Promotion of Science
[b] e-mail: nish@ynu.ac.jp

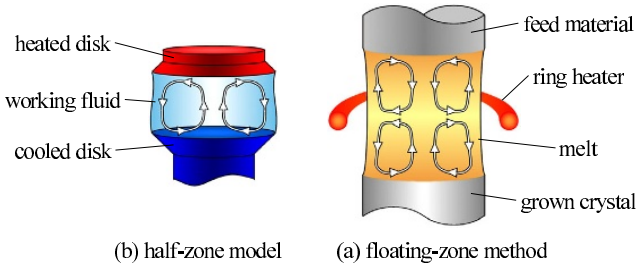

Fig. 1. Schematic of the (a) half-zone (HZ) liquid bridge and (b) floating-zone (FZ) liquid bridge.

et al. [2] found in their terrestrial experiments that the slenderness of the LB strongly affects the critical condition for unsteady Marangoni convection. Chen and Hu [3] and Kuhlmann et al. [4] also studied the effect of LB shape by means of the linear stability analysis. They reported that the Marangoni convection becomes most stabilized at a certain LB shape even for different experimental/numerical conditions such as disk diameter, working fluid and so on. Furthermore, Kuhlmann et al. [4] found that the critical azimuthal mode number is also affected by the LB shape, in agreement with the results from the previous ground based experiments [5–7].

The present study focuses on the effect of LB shape on the critical condition for the onset of oscillatory state and associated flow patterns. Obtained results are compared with the latest experimental benchmark reported by Shevtsova et al. [7]. The LB shape can be specified by the two dimensionless geometrical parameters. They are the aspect ratio, AR, and the volume ratio, VR, of the LB. The former is defined as $AR = H/D$, where H and D respectively denote the LB length and the disk diameter, while the latter is defined as $VR = V/V_0$, where V and V_0 respectively denote the LB volume and the cylindrical gap volume between upper and lower disks ($=\pi D^2 H/4$). The gravity causes the LB deformation and its effect is specified by the Bond number which is defined as $Bo = \Delta\rho g H^2/\sigma$, where $\Delta\rho$, σ and g are the density difference between liquid and gas, the surface tension and the acceleration of gravity, respectively. The effect becomes negligible for small LBs and in the microgravity environment. It is well known that the effects of AR and VR on the instability of thermal Marangoni convection appear not only in the critical temperature difference and oscillation frequency but also in the critical azimuthal mode number, which is denoted by m in this paper. The values of m should be integer because of the 2π-periodicity in the azimuthal direction of the LB. Preisser et al. [8] reported an experimentally observed relation of $AR \times m \approx 1.1$ for the LBs of $AR < 1.3$, $VR \approx 1.0$ and $Pr = 8.9$, where Pr is the Prandtl number. They showed that $m = 2$ for $AR = 0.55$ and $m = 1$ for $AR = 1.1$. Sakurai et al. [6] ($Pr = 16.0 \sim 68.4$) and Shevtsova et al. [7] ($Pr = 68$) studied the effects of AR and VR on m to find rather complex relations which were therefore reported in diagram or in tabular form. Lappa et al. [9] considered the effects of AR and VR to introduce the effective aspect ratio which is defined as $A_m = H/D_0$, where D_0 is chosen to be either minimum or maximum diameter of the LB in order to represent the slenderness or fatness of the LB. They suggested a modified empirical relation, $A_m \times m \approx 1$, from their numerical simulations for $AR = 0.25 \sim 1.25$, $VR = 0.78 \sim 1.22$ and $Pr = 0.01$ under zero gravity condition. This empirical relation was extended up to $Pr = 4$ by Nienhüser and Kuhlmann [10] by means of their linear stability analysis.

The present study aims at proposing a new dimensionless parameter that can be used for more general treatment of the effect of LB shape (i.e., AR and VR) on the instability of thermal Marangoni convection. As described later in this paper, the

Table 1. Physical properties of the test fluid at 25°C.

Test fluid	5cSt silicone oil
Prandtl number, Pr [-]	67
kinematic viscosity, ν [m^2/s]	5.0×10^{-6}
density, ρ [kg/m^3]	915
thermal diffusivity, α [m^2/s]	7.49×10^{-8}
surface tension, σ [N/m]	19.7×10^{-3}
temperature coefficient of σ, σ_T [N/(m·K)]	-6.58×10^{-5}
coefficient of thermal expansion, β [1/K]	1.09×10^{-3}

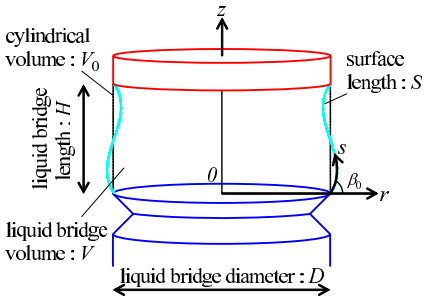

Fig. 2. Liquid bridge geometry.

surface length of LB is taken as a representative length scale, instead of H, to express the critical conditions and to define the dimensionless parameter. The surface length is evaluated from the LB shape that is calculated from the Young-Laplace equation [11]. It is demonstrated that not only the critical azimuthal mode number but also the critical conditions (i.e., the critical temperature difference and the oscillation frequency) can be correlated reasonably well by this new dimensionless parameter.

2 Method

2.1 Experimental conditions

Silicone oil with the kinematic viscosity of 5cSt at 25°C (Shin-Etsu Co., Ltd., KF-96L-5cs) is used as the test fluid (Pr=67). Typical physical properties of used fluid are listed in Table 1. The temperature dependency of ν is considerable thus it is evaluated from the following equation;

$$\nu(T) = \exp\left(5.892 \times \frac{25 - T}{273.15 + T}\right) \times \nu(25) \tag{1}$$

where T is the temperature in degree Celsius. The representative value of kinematic viscosity, $\bar{\nu}$, is evaluated as an average of those evaluated at the temperatures of heated disk and cooled disk (i.e., T_H and T_C). The working fluid is seeded with small tracer particles made of nylon-12 (Toray Industries, Inc., SP-500). Their average diameter and density are 5 μm and 1017 kg/m^3, respectively. The volume concentration of tracer particle is kept less than 0.05volume% so that their suspension does not affect the flow field.

The geometry of HZ LB is illustrated in Fig. 2. The diameters of both heated and cooled disks are 5 mm. The cooled disk has a 45° sharp edge to prevent the liquid

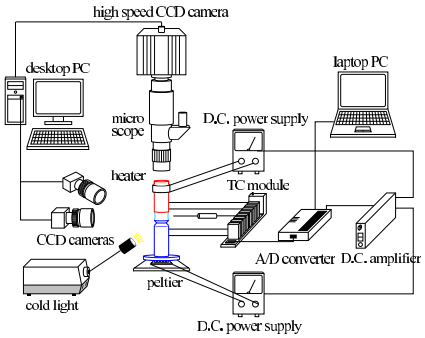

Fig. 3. Experimental setup.

leakage. Also to prevent fluid from creeping over the edges of upper and lower disks, they are covered with an anti-wetting-barrier. The lower cooled disk is traversed in axial (z) direction, so that AR is changed in the range of 0.50∼0.65. The resultant Bo changes from 2.84 to 4.80. VR is changed in the range of 0.6∼1.1. The ratio of buoyancy to thermocapillary forces is represented by the dynamic Bond number, which is defined as $Bd = \rho g \beta H^2/|\sigma_T|$, where ρ, β and σ_T are the density, the coefficient of thermal expansion and the temperature coefficient of surface tension, respectively. The resultant Bd changes from 0.93 to 1.57 for $AR = 0.50 \sim 0.65$. Masud et al. [2] showed from their experiments that the effect of buoyancy becomes negligible for Bd smaller than 0.26. Although $Bd = 0.93 \sim 1.57$ are larger than that, the present choice of $D = 5\,\text{mm}$ and $H = 2.5 \sim 3.25\,\text{mm}$ is the result of compromise between buoyancy and other factors such as evaporation, leakage, measurement resolution and so on.

2.2 Experimental setup

Schematic diagram of the experimental setup is shown in Fig. 3. The LB is formed between upper sapphire and lower aluminum disks. The temperatures of those disks are feedback controlled by the heating tapes and a Peltier device, respectively. Any required temperature difference between heated and cooled disks ($\Delta T = T_H - T_C$) can be realized stably.

In the present experiment, T_C is kept constant at 18°C within the accuracy of ±0.2°C and T_H is increased/decreased in a stepwise manner. The temperature signal measured by a fine thermocouple sensor placed near the liquid surface and the motion of tracer particles observed by CCD cameras are simultaneously used for the detection of oscillatory flow. The used thermocouple sensors sampled at 100 Hz, which is enough fast to detect the temperature fluctuation due to the flow instability. As shown in Fig. 3, three CCD cameras are mounted around the LB. Two CCD cameras (side-view cameras) observe the overall flow pattern and the LB shape from the orthogonal directions. Another high speed CCD camera with microscopic objective (top-view camera) observes the oscillation mode of Marangoni convection in radial plane through the transparent sapphire disk. Note that the main part of the experimental setup is surrounded with a rectangular plastic box to defend the LB from ambient air disturbance. It is known that the square amplitude of temperature signal, A^2, and its oscillation frequency, f, show a linear dependence on ΔT near the critical condition (Hopf bifurcation [12]). In this study, ΔT giving A^2=0 is obtained by using the linear approximation method and this extrapolated value is regarded as critical temperature difference, ΔT_c.

Table 2. Comparison of contact angle with benchmark [7] for $AR = 0.5$.

		$VR = 0.8$	$VR = 0.9$	$VR = 1.0$
$D = 3$mm, $Bo = 1.02$	benchmark	51.28°	67.98°	85.04°
	present	51.26°	67.99°	85.04°
$D = 5$mm, $Bo = 2.84$	benchmark	41.65°	58.95°	76.11°
	present	41.66°	58.94°	76.06°
$D = 6$mm, $Bo = 4.09$	benchmark	34.79°	52.56°	69.81°
	present	34.76°	52.55°	69.79°

The most important condition for the present study is to keep the liquid volume constant during the experiment. The LB is formed by using a lab-made apparatus which consists of micro syringe, fixture and micrometer head. The working fluid is supplied from the micro syringe, and the fluid volume is carefully adjusted with the micrometer head. The LB shape is always monitored with the side-view cameras and the lost volume due to the evaporation is compensated adequately. The minimum of adjustable fluid volume is $0.02\,\mathrm{mm}^3$, so the resolution is good enough for the present experiment (liquid volume for $AR = 0.5$, $VR = 1.0$ and $D = 5\,\mathrm{mm}$ is $V = 49.1\,\mathrm{mm}^3$). Detailed comparison of experimental and theoretical LB shape will be discussed in Sect. 3.1.

3 Result and discussion

3.1 Liquid bridge shape

For quantitative consideration of LB shape, the equilibrium LB shape is calculated from the Young-Laplace equation [11]. For the case of axisymmetric LB, it can be written as follows:

$$\frac{d^2r}{ds^2} = -\frac{dz}{ds}\left(-\frac{Bo}{AR^2}\frac{z}{D^2} + \frac{C}{\sigma} - \frac{1}{r}\frac{dz}{ds}\right) \tag{2a}$$

$$\frac{d^2z}{ds^2} = \frac{dr}{ds}\left(-\frac{Bo}{AR^2}\frac{z}{D^2} + \frac{C}{\sigma} - \frac{1}{r}\frac{dz}{ds}\right) \tag{2b}$$

where s, r, z and C are respectively the curve arc length, the radial position, the axial position and the constant which depends on the pressure difference between liquid and air. Note that r and z are the function of s. In the followings, the values of $9.8\,\mathrm{m/s}^2$ and $1.18\,\mathrm{kg/m}^3$ are used for the acceleration of gravity and the density of air, respectively. The problem can be solved numerically as an initial value problem by using shooting method [11]. The boundary conditions are as follows: (1) $r = D/2$ at $z = 0$, H, (2) $dr/ds = \cos\beta_0$, $dz/ds = \sin\beta_0$ at $s = 0$ and (3) $\pi \int r^2 dz = VR \times V_0$, where β_0 is the contact angle at lower disk edge (Fig. 2). The calculated results are verified with the benchmark results reported by Shevtsova et al. [7] in terms of contact angle at the upper disk. The detailed values are summarized in Table 2 with good agreement, indicating that the Young-Laplace equation is solved successfully.

Figure 4 shows the LBs for different VR and constant $AR(= 0.50)$. The LBs are illuminated from the backside, and it makes easier to detect the interface between liquid and air. The resultant shapes of liquid surface are compared with those obtained from Eq. (2) in Fig. 5. There is reasonable agreement between experiment and calculation. Their differences of VR are less than 1%, indicating that accurate

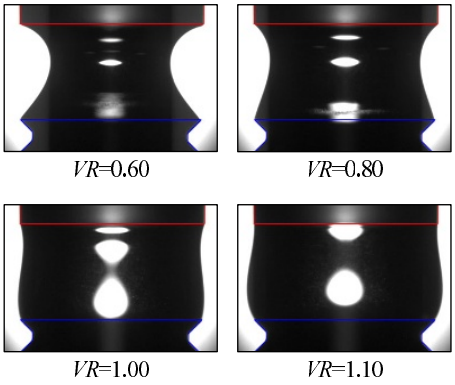

Fig. 4. Variety of liquid bridge shapes for $AR = 0.5$.

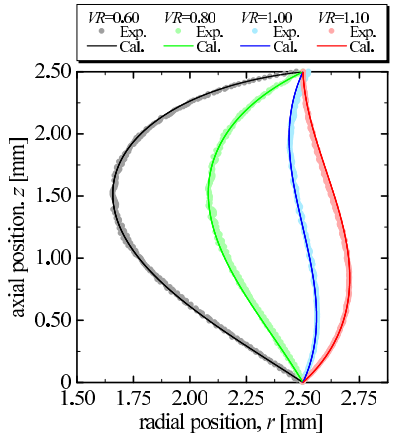

Fig. 5. Comparison of liquid bridge shapes between experiment and calculation.

evaluation of VR can be realized in the present study. As a result, the surface length of LB, denoted by S (Fig. 2), which is the tangential length of LB from the cooled disk to the heated disk, is evaluated from the calculated LB shape.

3.2 Instability of Marangoni convection

In this study, ΔT_c, f and associated oscillation modes are measured for various combinations of AR and VR. For the better understanding, obtained ΔT_c and f are non-dimensionalized into Marangoni number, Ma_H, and dimensionless oscillation frequency, F_H [8], which are defined as follows;

$$Ma_H = \frac{|\sigma_T|\Delta T H}{\rho \bar{\nu} \alpha} \tag{3}$$

$$F_H = \frac{H^2}{\alpha \sqrt{Ma_H}} f \tag{4}$$

where α is the thermal diffusivity. The Ma_H with $\Delta T{=}\Delta T_c$ gives a critical Marangoni number, Ma_{cH}. Figure 6 shows the measured (a) Ma_{cH} and (b) F_H as a function of

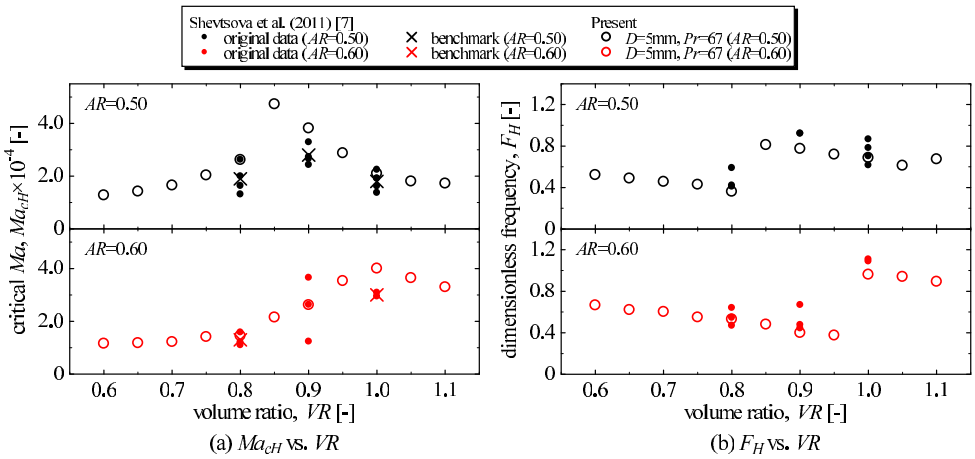

Fig. 6. Plot of (a) Ma_{cH} and (b) F_H as a function of VR comparing with the benchmark results [7].

VR for AR=0.50 (upper) and 0.60 (lower). Also included in these results are the experimental benchmarks reported by Shevtsova et al. [7]. They presented the benchmark values of Ma_{cH} which are obtained from nine test cases conducted by five different groups. Their liquid volume was changed for $VR = 0.80$, 0.90 and 1.00 for each AR(= 0.32, 0.50 and 0.60) whereas the results for $AR = 0.32$ is not discussed here because ΔT_c for this AR becomes too high to be measured in the present study. Note that the data for $AR = 0.60$ and $VR = 0.90$ are not available from the benchmark. The results of Ma_{cH} show a reasonable agreement between the present experiment and the benchmark however all measured values in the present experiment are slightly larger than the benchmarks. It is well known that the onset condition of oscillatory Marangoni convection is very sensitive to the boundary conditions, and such a slight discrepancy may be caused by the difference of experimental conditions. In Fig. 6, there are two branches of stability curve which can be assigned to larger/smaller VR, and they appear to intersect with each other at quite high Ma_{cH} condition. As shown later, their meeting point is found to be corresponding to the transition point of m and therefore F_H shows a jump at this condition (Fig. 6b). Here, oscillatory flows with $m = 1$ appears for smaller VR and those with $m = 2$ appears for larger VR. As for F_H, the present experiment and the previous data are in good agreement, thus supporting again the appropriateness of the present experiment.

Figure 7 shows the plots of (a) Ma_{cH} and (b) F_H as a function of VR for different ARs ($AR = 0.50$, 0.55, 0.60 and 0.65). The Ma_{cH}–VR plot for each AR show a local peak at a certain VR, at which the F_H–VR plot for corresponding AR shows a sudden increase. More importantly, a definite transition of m occurs at this VR as recognized from the open symbols ($m = 1$) and the closed symbols ($m = 2$) in both plots. This particular VR is, therefore, referred to as the mode-transition VR hereafter. It is obvious that the mode-transition VR increases with AR in the range studied here. It is reported that the mode-transition VR also depends on Bo and the surrounding conditions in the air near the interface [7]. From Figs. 7a and 7b, each dependence of Ma_{cH} and F_H on AR for constant VR can be interpreted as follows: (1) Ma_{cH} decreases while F_H increases with AR for small VR (say, $VR < 0.8$) where $m = 1$, and (2) both Ma_{cH} and F_H increase with AR for large VR (say, $VR > 1.0$) where $m = 2$. This interpretation suggests that the dependence of instability of thermal Marangoni convection on AR and VR can be simplified by introducing a new dimensionless parameter that can specify the mode transition caused by the change of AR and VR.

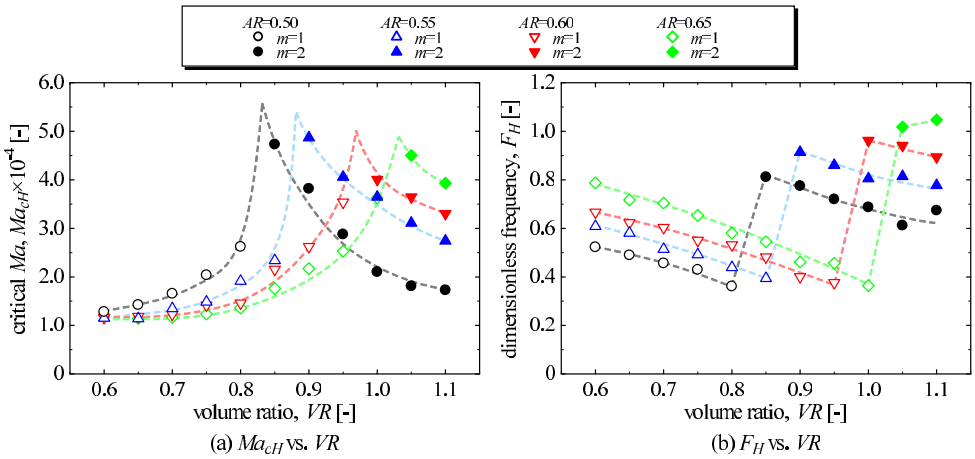

Fig. 7. Plot of (a) Ma_{cH} and (b) F_H as a function of VR with various AR.

3.3 New dimensionless parameter

In the former section, it is suggested that the trends of Ma_{cH}, F_H and m strongly depend on both AR and VR. The purpose of this section is to propose a new dimensionless parameter with a view to correlating the complex dependence of the critical conditions on AR and VR into simpler relations. Considering that the driving force of thermal Marangoni convection is exerted on the LB surface, S is used, instead of H, as a characteristic length for defining the Marangoni number and the dimensionless oscillation frequency. Furthermore, S is used to define a dimensionless parameter, SDR $(= S/D_0)$, which is to describe the LB shape, where D_0 is the minimum or maximum diameter of the LB as considered by Masud et al. [2] and Lappa et al. [9]. For deformed LBs that exhibit both concave and convex surfaces, D_0 is defined as an average of the minimum and the maximum diameter of the concave and the convex surfaces, respectively, as proposed by Masud et al. Although intuitively introduced, S and SDR are shown to be quite useful for the correlation of the dependence of the critical conditions on the LB shape.

Figure 8 shows the relation of SDR, VR and AR, where open symbols and closed symbols represent the critical modes of $m = 1$ and $m = 2$, respectively. It is evident that $SDR \approx 0.64$ corresponds to the mode transition from the $m = 2$ to $m = 1$. This mode transition at $SDR \approx 0.64$ holds true for the data of Preisser et al. [8] ($Pr = 8.9$) and Shevtsova et al. [5] ($Pr = 105$). The former reported $m = 1$ for $AR = 0.7 \sim 1.2$ (corresponding to $SDR = 0.7 \sim 1.2$) and $m = 2$ for $AR = 0.4 \sim 0.65$ ($SDR = 0.4 \sim 0.65$), both for $VR \approx 1.0$, while latter reported $m = 1$ for $VR = 0.7 \sim 0.95$ ($SDR = 0.64 \sim 0.97$) and $m = 2$ for $VR = 1.05 \sim 1.2$ ($SDR = 0.59 \sim 0.61$), both for $AR = 0.6$. Note that $Bd = 0.7 \sim 2.9$ for the data of Preisser et al. while $Bd = 2.3$ for the data of Shevtsova et al. These results indicate that the complex dependence of m on AR and VR can be simplified by use of SDR, at least for the available data taken in the ground experiments.

Figure 9 shows (a) the critical Marangoni number, Ma_{cS}, and (b) the dimensionless oscillation frequency, F_S, plotted as a function of SDR, where S is used as the characteristic length in Eqs. (3) and (4) instead of H. The figures show reasonable correlations of Ma_{cS} and F_S with SDR, demonstrating the usefulness of SDR. These figures clearly show the presence of two branches corresponding to $m = 1$ and 2. As for Ma_{cS}, the stability curves for m=2 and 1 appear to be intersected to each other, showing a sharp peak of Ma_{cS} ($\approx 5.0 \times 10^4$) at $SDR \approx 0.64$ and an asymptotic

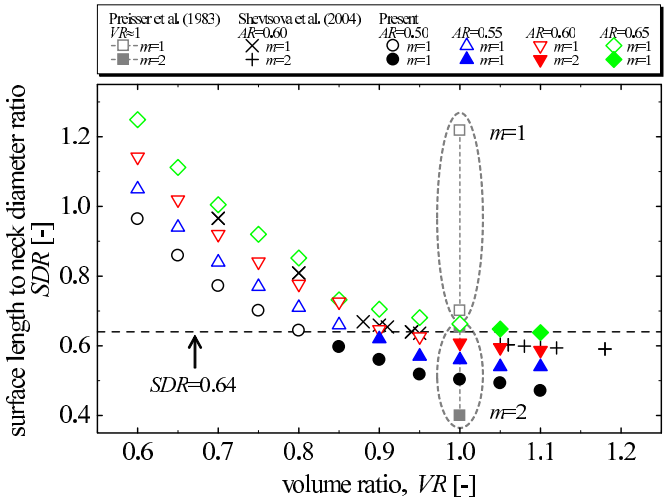

Fig. 8. Relation of SDR and VR for various AR.

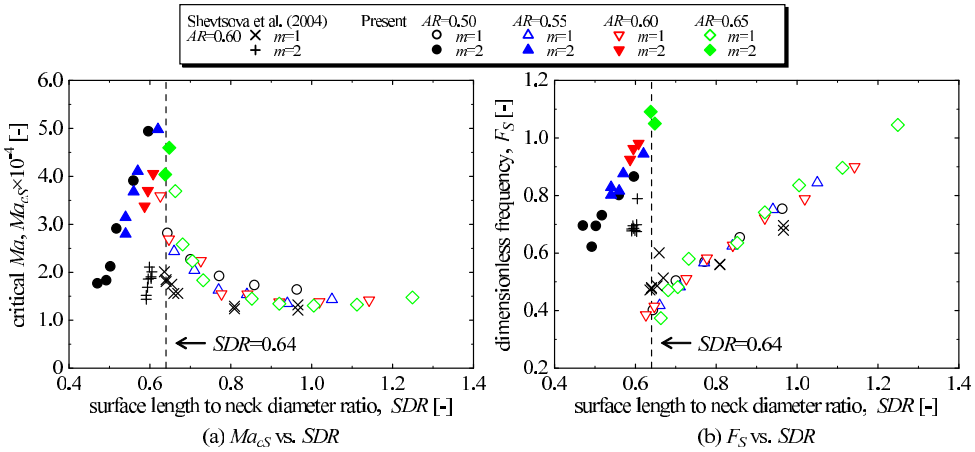

(a) Ma_{cS} vs. SDR (b) F_S vs. SDR

Fig. 9. Plot of (a) Ma_{cS} and (b) F_S as a function of SDR.

approach to a value ($\approx 1.5 \times 10^4$) with increasing SDR. On the other hand, F_S shows two linear branches revealing a discontinuous decrease at $SDR \approx 0.64$. These correlations of Ma_{cS} and F_S with SDR appear to be in agreement with the data reported by Shevtsova et al. [5], except for the values Ma_{cS} near $SDR = 0.64$ where the mode transition takes place and therefore Ma_{cS} could be sensitive to each experimental conditions.

4 Conclusions

The present paper reports the effect of liquid bridge shape on the instability and associated oscillation mode of thermal Marangoni convection in liquid bridges of 5cSt silicone oil. The shape is varied in the ranges of $AR = 0.50 \sim 0.65$ and $VR = 0.60 \sim 1.10$ for a single disk diameter of 5 mm. The liquid volume is controlled accurately by using a lab-made micro syringe apparatus. The measured liquid bridge shapes compare well with those calculated from the Young-Laplace equation. Onset conditions of

oscillatory state, oscillation frequencies and associated oscillation modes are determined experimentally. The results plotted as a function of VR reveal the presence of local peak of critical Marangoni number and the presence of a suddenly decrease of oscillation frequency at a certain VR. The position of this peak shifts with AR and the observed azimuthal mode number changes at this peak position. To correlate the complex effect of AR and VR in a simple way, a new dimensionless parameter SDR is proposed. It is the ratio of the liquid surface length to the neck diameter of the liquid bridge. It is shown that the transition of azimuthal mode numbers (i.e., the transition from $m = 2$ to $m = 1$) for all ARs and VRs examined here takes palce at $SDR \approx 0.64$. It is also shown that the critical Marangoni numbers and the dimensionless oscillation frequencies fall onto their respective curve, if they are non-dimensionalized with the liquid surface length instead of the liquid bridge height. Each curve consist of two branches, one is stability curve for $m = 1$ and the other for $m = 2$. The tendencies of the critical Marangoni number and the dimensionless oscillation frequency change at the crossing point of these two branches. The usefulness of SDR is further checked by the reasonable agreement between the present results and the literature data.

This study was supported by Japan Society for the Promotion of Science (JSPS) KAKENHI (Grant-in-Aid for JSPS Fellows, 13J02728 and Grant-in-Aid for Scientific Research (B), 24360078).

References

1. W.R. Hu, J.Z. Shu, R. Zhou, Z.M. Tang, J. Cryst. Growth **142**, 379 (1994)
2. J. Masud, Y. Kamotani, S. Ostrach, J. Thermophys. Heat Transfer **11**, 105 (1997)
3. Q.S. Chen, W.R. Hu, Int. J. Heat Mass Transfer **41**, 825 (1998)
4. H.C. Kuhlmann, C. Nienhüser, H.J. Rath, S. Yoda, Adv. Space Res. **29**, 639 (2002)
5. V.M. Shevtsova, M. Mojahed, D.E. Melnikov, J.C. Legros, in *Interfacial Fluid Dynamics and Transport Processes*, edited by R. Narayanan, D. Schwabe, Lecture Notes in Physics, Vol. 628 (Springer, Berlin, Heidelberg, 2003), p. 240
6. M. Sakurai, N. Ohishi, A. Hirata, J. Cryst. Growth **308**, 360 (2007)
7. V. Shevtsova, A. Mialdun, H. Kawamura, I. Ueno, K. Nishino, M. Lappa, Fluid Dynam. Mater. Process. **7**, 1 (2011)
8. F. Preisser, D. Schwabe, A. Scharmann, J. Fluid Mech. **126**, 545 (1983)
9. M. Lappa, R. Savino, R. Monti, Int. J. Heat Mass Transfer **44**, 1983 (2001)
10. Ch. Nienhüser, H.C. Kuhlmann, J. Fluid Mech. **458**, 35 (2002)
11. L.A. Slobozhanin, J.M. Perales, Phys. Fluids A **5**, 1305 (1993)
12. D. Schwabe, Phys. Fluids **17**, 112104 (2005)